Involvement of phosphatidylinositol 4,5-bisphosphate in RNA polymerase I transcription

Sukriye Yildirim[1,*], Enrique Castano[1,2,*], Margarita Sobol[1], Vlada V. Philimonenko[1], Rastislav Dzijak[1], Tomáš Venit[1] and Pavel Hozák[1,‡]

[1]Laboratory of Biology of the Cell Nucleus, Institute of Molecular Genetics ASCR, v.v.i., Vídeňská 1083, 142 20, Prague 4, Czech Republic
[2]Biochemistry and Molecular Plant Biology Department, CICY, Calle 43, No.130, Colonia Chuburná de Hidalgo C.P. 97200, Mérida, Yucatán, México

*These authors contributed equally to this work
‡Author for correspondence (hozak@img.cas.cz)

Accepted 16 March 2013
Journal of Cell Science 126, 2730–2739

doi: 10.1242/jcs.123661

Summary

RNA polymerase I (Pol I) transcription is essential for the cell cycle, growth and protein synthesis in eukaryotes. In the present study, we found that phosphatidylinositol 4,5-bisphosphate (PIP2) is a part of the protein complex on the active ribosomal promoter during transcription. PIP2 makes a complex with Pol I and the Pol I transcription factor UBF in the nucleolus. PIP2 depletion reduces Pol I transcription, which can be rescued by the addition of exogenous PIP2. In addition, PIP2 also binds directly to the pre-rRNA processing factor fibrillarin (Fib), and co-localizes with nascent transcripts in the nucleolus. PIP2 binding to UBF and Fib modulates their binding to DNA and RNA, respectively. In conclusion, PIP2 interacts with a subset of Pol I transcription machinery, and promotes Pol I transcription.

Key words: Nucleolus, Transcription, PIP2, UBF, Fibrillarin

Introduction

The eukaryotic nucleus is a highly structured organelle composed mainly of proteins and nucleic acids. However, in addition to these abundant molecules, the nuclear interior was also shown to contain minor components such as lipids (Rose and Frenster, 1965). Several biochemical studies (Boronenkov et al., 1998; Cocco et al., 1987; Divecha et al., 1991; Vann et al., 1997) have shown that purified nuclei contain enzymes involved in the production and degradation of phosphoinositides (PI). These studies also suggested that PIs could be divided into physically separate pools within the nucleus. Initial experiments with the antibody against phosphatidylinositol 4,5-bisphosphate (PIP2) and the pleckstrin homology domain of phospholipase C δ1 (PLCδ1PH) as probes (Osborne et al., 2001; Watt et al., 2002) revealed the presence of their cognate lipid in distinct nuclear compartments such as the interchromatin granule clusters and the nucleolus. While there have been no reports on the function of nucleolar PIP2, a number of studies have shown PIP2 function in nuclear speckles (Boronenkov et al., 1998; Mellman et al., 2008; Osborne et al., 2001). Phosphatidylinositol-4-phosphate 5-kinase, type 1 alpha and a non-canonical poly (A) polymerase, called Star-PAP, were detected in the nuclear speckles where 3′-end processing of select mRNAs by Star-PAP was stimulated by PIP2 (Mellman et al., 2008). PIP2 immunodepletion from HeLa nuclear extracts caused inhibition of precursor mRNA splicing due to the loss of PIP2 and its binding partners (Osborne et al., 2001). Moreover, apart from mRNA processing, mRNA export was also shown to be regulated by PIP2 in speckles. PIP2 binding to the mRNA export protein Aly directed the protein to nuclear speckles, while the disruption of PIP2 binding caused a reduction in its mRNA export activity (Okada et al., 2008). A few studies showed the involvement of PIP2 in RNA polymerase II (Pol II) transcription. In *Drosophila*, PIP2 binding to histone H1 reversed the inhibitory effect of histone H1 on transcription (Yu et al., 1998). Similarly, a Drosophila trithorax group protein, ASH2, binding to nuclear phosphatidylinositol 4-phosphate 5-kinase, called SKTL, was shown to be involved in maintaining transcriptionally active chromatin via reducing histone H1 hyperphosphorylation (Cheng and Shearn, 2004). In mammalian cells, PIP2 was found to bind only the hyperphosphorylated active form of Pol II (Pol IIO), implying its role in Pol II transcription (Osborne et al., 2001). PIP2 was required for activation of SWI-SNF like BAF complex binding to nuclear matrix/chromatin in actin-dependent manner (Zhao et al., 1998). PIP2 also facilitated the synthesis of filamentous actin in the nucleus by interfering with BRG1-actin binding at the C-terminus of BRG1 (Rando et al., 2002). Even though PIP2 presence was shown in the nucleolus (Mortier et al., 2005; Osborne et al., 2001), nucleolar PIP2 function has not been yet investigated. The nucleolus is composed of well-defined subdomains such as fibrillar centers (FCs), a dense fibrillar component (DFC), and a granular component (GC). Transcription of pre-ribosomal genes takes place at the FC/DFC border while ribosomal subunits assemble in the GC (Németh, Längst, 2011). Nucleoli are formed around nucleolar organizer regions (NORs), which contain tandem rRNA gene repeats. Each ribosomal gene unit usually consists of a transcribed sequence and an external non-transcribed spacer (Liau and Perry, 1969). Even though 400 copies of rDNA exist in diploid somatic cells, only a small fraction is transcribed and the transcription is driven by Pol I upon binding to UBF together with the SL1 complex at the enhancer region of rDNA. UBF binds to rDNA not only at the promoter, but also in the transcribed region, and it is involved in the formation of open

chromatin structures at actively transcribed genes (Denissov et al., 2011). Since UBF recruitment to UBF-binding site arrays outside the nucleolus forms pseudo-NORs (Mais et al., 2005), it is suggested that UBF is involved in structural organization of rDNA for the assembly of FC and DFC regions.

Upon transcription initiation, rRNA transcripts proceed through several maturation stages before ribosomal subunit assembly (Mayer and Grummt, 2006). In the early stages of rRNA processing, Fib, being a component of ribonucleoprotein complex called box C/D small nucleolar RNP, binds to precursor rRNA in the DFC region and functions in site-specific 2′-*O*-methylation of rRNA (Hernandez-Verdun, 1991). Mutations affecting Pol I elongation also have an effect on precursor rRNA cleavage by the Spt4–Spt5 complex in yeast linking both machineries (Anderson et al., 2011; Schneider et al., 2006; Schneider et al., 2007). Fib is recruited to nucleoli upon transcription initiation in telophase, and its presence at this point of the cell cycle was shown to be essential for cell survival (Dundr et al., 1997; Kopp et al., 2007).

Here we document that PIP2 interacts directly or indirectly with Pol I in the nucleolus. We also show that direct binding of PIP2 to UBF and Fib may change their respective conformation and thus the ability to bind nucleic acids. Moreover, nascent rRNAs co-localize with PIP2 *in vivo*, and *in vitro* ribosomal gene transcription is compromised when PIP2 is depleted. Addition of exogenous PIP2 can rescue the transcription inhibition while exogenous IP3 [Ins (1,4,5)P3] and DAG have no effect. Pre-incubation with anti-PIP2 antibodies and PIP2 depletion by addition of PLC before transcription initiation abolishes nucleolar transcription. These results indicate that PIP2 might be involved in Pol I transcription by interacting with pre-rRNA production and processing machineries.

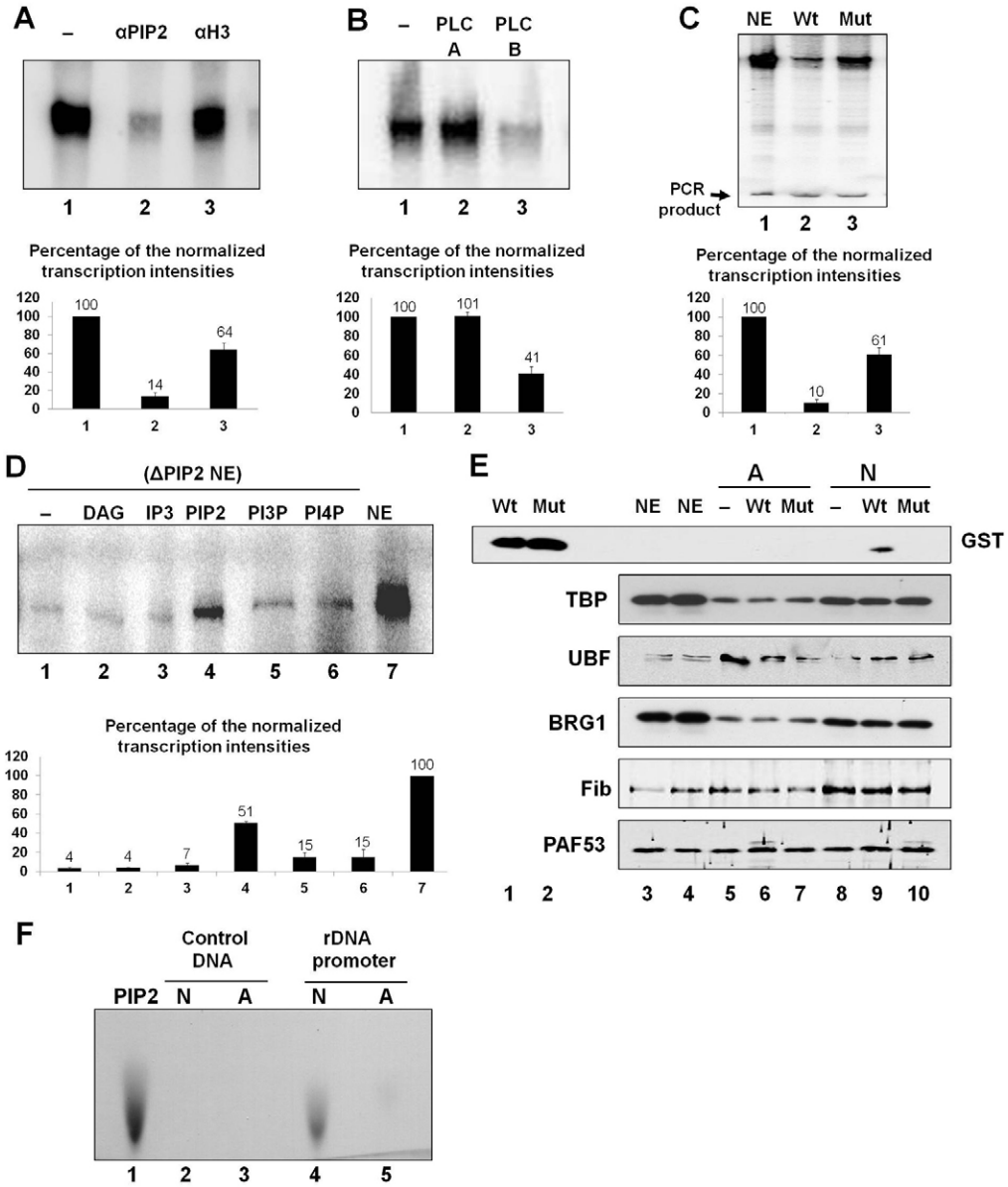

Fig. 1. See next page for legend.

Results

PIP2 is required for optimal Pol I transcription *in vitro*

On the basis of existing evidence suggesting involvement of PIP2 in Pol II transcription (Yu et al., 1998), we investigated PIP2 influence on Pol I transcription using several strategies for *in vitro* transcription assays. When anti-PIP2 antibody was added to *in vitro* transcription assay, the level of Pol I transcription was reduced by more than 80% (Fig. 1A, lane 2). On the other hand, anti-histone H3 antibody, which was used as a control antibody at similar concentration, had a minor inhibitory effect on transcription (Fig. 1A, lane 3). It was possible to neutralize the inhibitory effect of anti-PIP2 antibody in transcription by pre-blocking the antibody with PIP2 before its addition to the transcription reaction in a dose-dependent manner (supplementary material Fig. S1). We then tested if degradation of existing nuclear PIP2 by phospholipase C (PLC) enzyme has an effect on transcription. Indeed, the addition of purified PLC to the nuclear extract prior to transcription initiation (before the addition of nucleotides) caused almost 60% inhibition in transcription, while the addition of the PLC at the time of transcription initiation (after the addition of nucleotides) showed no significant effect as seen in Fig. 1B. To further test the effect of PIP2 on transcription we compared Pol I transcription levels using nuclear extracts in which PIP2 was depleted using GST-tagged PLCδ1PH domain. The PLCδ1PH domain binds to the PIP2 head group with a high affinity and a single basic amino acid replacement in the N-terminal part of the domain (R40A) results in the abolishment of PIP2 binding (Yagisawa et al., 1998). When PLCδ1PH domain was added to the nuclear extract, Pol I transcription was reduced significantly as compared with nuclear extract where PIP2-binding mutant PLCδ1PH domain was added (Fig. 1C). PIP2 cleavage by nuclear PLCs results in the production of second messengers (IP3 and DAG) in the nucleus (for review see Irvine, 2003). In order to confirm that PIP2 or products of PIP2 cleavage are the executive molecules in Pol I transcription modulation, PIP2, IP3 or DAG were added into PIP2 depleted extract and used for *in vitro* transcription assays. While IP3 and DAG addition showed no effect on transcription, PIP2 addition significantly restored (~50%) Pol I transcription in PIP2-depleted extracts However, PI3P or PI4P addition resulted in only 15% increase in transcription (Fig. 1D). These results clearly show that PIP2 acts in Pol I transcription directly, but not as a source for second messengers. The PIP2 presence on the promoter along with the transcription machinery was checked at different stages of transcription using the rDNA promoter bound to magnetic beads. Addition of GST-tagged PLCδ1PH domain to the transcription reaction showed the presence of PIP2 at the transcription machinery on the promoter when successful transcription was achieved by the addition of all four rNTPs (N) as shown in Fig. 1E, lane 9. Alternatively, when only ATP (A) was added to the transcription mixtures during transcription preinitiation to promote the phosphorylation required before the transcription, there was no detectable PIP2 level on the promoter as seen in Fig. 1E, lane 6. When PIP2-binding mutant PLCδ1PH domain was added to the transcription reaction, there was no staining with anti-GST antibody, indicating the inability of mutant domain to bind to PIP2 (Fig. 1E, lanes 7 and 10). The amounts of Fib, BRG1 and TBP on the promoter were ~2× higher during transcription compared with preinitiation reactions. The presence of PIP2 in transcription complexes on the promoter region was also directly shown in TLC after lipid extraction (Fig. 1F). In summary, this is the first report showing that PIP2 is a part of Pol I transcription machinery on the promoter and promotes Pol I transcription *in vitro*.

Fig. 1. PIP2 promotes Pol I transcription *in vitro*. (**A**) Run-off transcription reaction showed that addition of anti-PIP2 antibody (clone 2C11, Abcam, Cambridge, UK; 0.8 μg) decreases transcription levels by more than 80%. On the other hand, anti-histone H3 antibody (H0164, Sigma Aldrich, St. Louis, MO, USA; 0.5 μl) had a minor effect on Pol I transcription. (Lane 1, control transcription reaction; lane 2, transcription reaction in the presence of anti-PIP2 antibody; lane 3, transcription reaction in the presence of anti-histone H3 antibody.) The chart shows relative activities (mean±s.e.m.) normalized to an internal DNA control from two independent experiments. (**B**) The effect of PLC enzyme on *in vitro* transcription is shown. PLC (100 ng) addition before the addition of nucleotides (PLC B) inhibited Pol I transcription, whereas PLC addition after the addition of nucleotides (PLC A) did not inhibit transcription. (Lane 1, control transcription reaction; lane 2, transcription reaction in the presence of PLC added after nucleotides; lane 3, transcription reaction in the presence of PLC added before nucleotides.) The chart shows relative activities (mean±s.e.m.) normalized to an internal DNA control from two independent experiments (**C**) Nuclear extracts (NE) were depleted for PIP2 using PLCδ1PH coated beads. As a control, PLCδ1PH-Mut coated beads were used for depletion, since PLCδ1PH-Mut fails in binding to PIP2 (Yagisawa et al., 1998). Transcription intensities were normalized by 700 bp PCR product labeled with [α-^{32}P]. PIP2 depletion by PLCδ1PH domain caused 90% inhibition in transcription, whereas mutant domain did not show such a pronounced inhibitory effect (~40% inhibition). (Lane 1, non-depleted nuclear extract; lane 2, nuclear extract depleted with PLCδ1PH; lane 3, nuclear extract depleted with PLCδ1PH-Mut domain.) The chart shows relative activities (mean±s.e.m.) normalized to an internal DNA control from two independent experiments (**D**) PIP2-depleted nuclear extracts supplemented with DAG, IP3, PIP2, PI3P and PI4P were tested for Pol I transcription. PIP2 supplementation resulted in the most dramatic rescue of transcription compared with other compounds tested. (Lane 1, PIP2-depleted nuclear extract; lane 2, PIP2-depleted nuclear extract supplemented with DAG (100 ng); lane 3, PIP2-depleted nuclear extract supplemented with IP3 (100 ng); lane 4, PIP2-depleted nuclear extract supplemented with PIP2 (100 ng); lane 5, PIP2-depleted nuclear extract supplemented with PI3P (100 ng); lane 6, PIP2-depleted nuclear extract supplemented with PI4P (100 ng); lane 7, non-depleted control nuclear extract.) The chart shows relative activities (mean±s.e.m.) normalized to an internal DNA control from two independent experiments. (**E**) In order to visualize PIP2 during transcription; we used rDNA promoter bound to Dynabeads. GST-tagged Wt or Mut PLCδ1PH domains were purified from bacteria, added to *in vitro* transcription mixtures and probed with anti-GST antibody. There was no detectable binding of Wt PLCδ1PH domain to the promoter in the presence of ATP solely, and only after the addition of all four rNTPs was binding detected, indicating that PIP2 binds to the promoter region only when transcription is active, *in vitro*. (Lane 1, PLCδ1PH domain; lane 2, PLCδ1PH-Mut domain; lanes 3 and 4, nuclear extract; lane 5, transcription reaction in the presence of ATP; lane 6, transcription reaction with ATP and PLCδ1PH domain; lane 7, transcription reaction with ATP and PLCδ1PH-Mut domain; lane 8, transcription reaction in the presence of all four rNTPs; lane 9, transcription reaction with rNTPs and PLCδ1PH domain; lane 10, transcription reaction with rNTPs and PLCδ1PH-Mut domain.) (**F**) In order to prove the presence of PIP2 at the transcription machinery on the promoter during transcription, we used rDNA promoter bound to Dynabeads. PIP2 was found on the rDNA promoter upon the addition of all four rNTPs [N] but not on the control DNA after extracting the lipids with chloroform/methanol/HCl and analyzing them by TLC. (Lane 1, purified PIP2; lanes 2 and 4, lipids from transcription reactions with all four rNTPs; lanes 3 and 5, lipids from *in vitro* transcription reactions with only ATP added.) Lipids were stained with acidic phosphomolybdate solution.

PIP2 participates in the formation of Pol I transcription foci

PIP2 presence in the nucleolus has been previously shown by Osborne et al. (Osborne et al., 2001) and Mortier et al. (Mortier et al., 2005); however, there has been no report on the interacting partners and functions of nucleolar PIP2. Since PIP2 was found to be a part of the transcription machinery on the promoter during rDNA transcription, we continued to identify the components of Pol I transcription machinery that interact with PIP2. For this purpose, GST-tagged PLCδ1PH domain and its PIP2-binding mutant were added to the nuclear extract and pulled down by glutathione beads. Since wild type PLCδ1PH domain can bind to PIP2, but not the mutant form, proteins pulled down by only wild type PLCδ1PH domain were considered as interacting partners of PIP2. As a second approach, PIP2-coupled agarose beads and control agarose beads were used for pull-down experiments. For microscopy studies, anti-PIP2 antibody or GST-tagged PLCδ1PH domain and anti-GST antibody were used. The use of recombinant PLCδ1PH domain as a PIP2 probe provided a reliable and consistent staining of PIP2 on the plasma membrane (Fig. 2A) and in the nucleus and nucleolus (Fig. 2B), while the mutant PLCδ1PH domain which does not bind to PIP2 did not provide a signal with immunofluorescent staining (Fig. 2B), thus proving the specificity of PLCδ1PH domain binding.

Pull-downs with PLCδ1PH domain showed that PIP2 and the largest subunit of Pol I (RPA116) are present in the same complex (Fig. 2C; supplementary material Fig. S2). In agreement, the immunofluorescence detection in U2OS cells showed PIP2 in concrete foci in the nucleolus together with Pol I (Fig. 2D). The co-localization of PIP2 and Pol I is documented by the intensity profile showing that fluorescence maxima of both proteins along the line crossing nucleolus clearly coincide (Fig. 2D). On the other hand, TBP and TAF 95/110 which are also members of transcription initiation machinery were not detected in the protein complex along with PIP2 (Fig. 2E; supplementary material Fig. S3), indicating that PIP2 interacts with a subset of proteins of Pol I transcription machinery. This selective composition of PIP2-bound protein complex is also reflected in PIP2 localization in the nucleolus. Fib is localized to DFC where transcription takes place while B23 is localized in GC where ribosomal subunits assemble (Németh, Längst, 2011). Since Fib is present in PIP2–protein complex and B23 is absent (Fig. 2E), we suggest that the restricted PIP2 localization to the transcriptionally active sites of the nucleolus might be dictated by the binding partners of PIP2.

UBF and Fib are both essential components of rRNA biogenesis during Pol I transcription initiation and early steps of rRNA maturation, respectively. We pulled both of them down from nucleolar extracts via PIP2-coupled agarose beads (Fig. 3A; supplementary material Fig. S4). After checking the specificity of the antibodies (supplementary material Fig. S5), co-localization studies of PIP2 with UBF and Fib were performed. PLCδ1PH domain showed a prominent co-localization of PIP2 with UBF and Fib in the nucleoli of interphase cells as documented by the corresponding intensity profiles (Fig. 3B). In addition, super-resolution structured illumination microscopy (SIM) allowed us to demonstrate PIP2 co-localization with UBF and Fib in

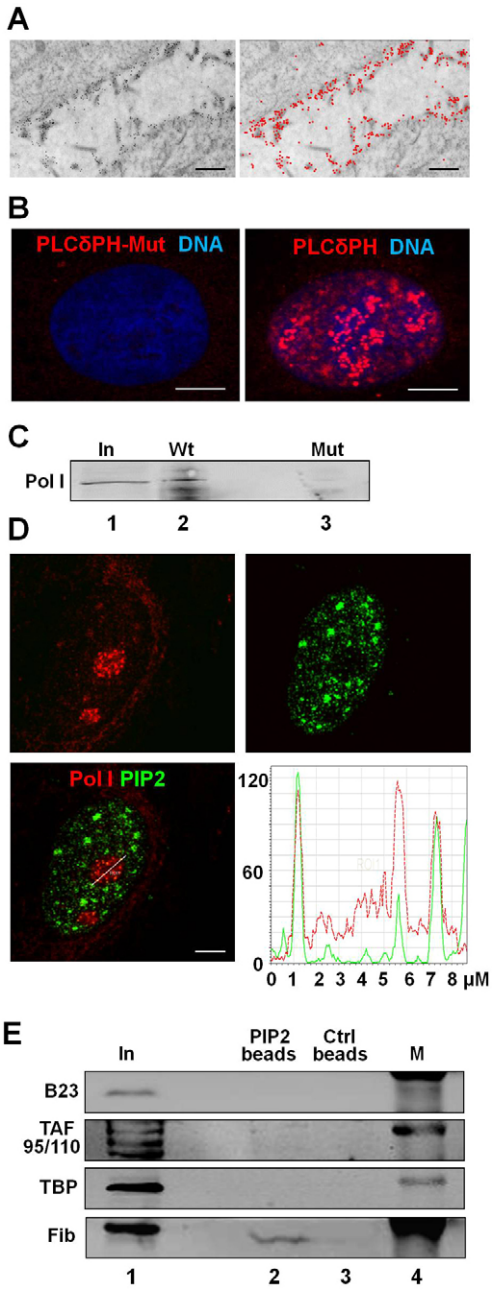

Fig. 2. PIP2 binds to the largest subunit of Pol I. In order to test the suitability of PLCδ1PH domain for PIP2 detection, we performed ultrastructural immunolabeling and immunofluorescence. (**A**) Immunogold electron microscopy was carried out using PLCδ1PH domain as a PIP2 sensor. PIP2 was localized at the plasma membrane of HeLa cells as expected. Scale bars: 500 nm. (**B**) There is no staining in the nucleus when U2OS cells are incubated with PLCδ1PH-Mut domain as a control. Scale bars: 5 µm. (**C**) PLCδ1PH domain pulled down RPA116 *in vitro* but the Mut form of PLCδ1PH domain failed to pull down RPA116. (Lane 1, input; lane 2, protein pulled down with Wt PLCδ1PH domain; lane 3, protein pulled down with Mut PLCδ1PH domain.) (**D**) *In vivo*, anti-PIP2 antibody showed co-localization with Pol I subunit RPA 116 in nucleoli of U2OS cells. Scale bar: 5 µm. (**E**) Nuclear extract was incubated with agarose beads coupled to PIP2 in order to pull down proteins interacting with PIP2. Pol I transcription machinery and nucleolar proteins were checked in the pull-down and fibrillarin was found to be present, whereas B23, TAF 95/110 and TBP were absent from the PIP2–protein complex. (Lane 1, input; lane 2, pull-down with PIP2-coupled agarose beads; lane 3, pull-down with control agarose beads; lane 4, marker.) In, input; Ctrl, control.

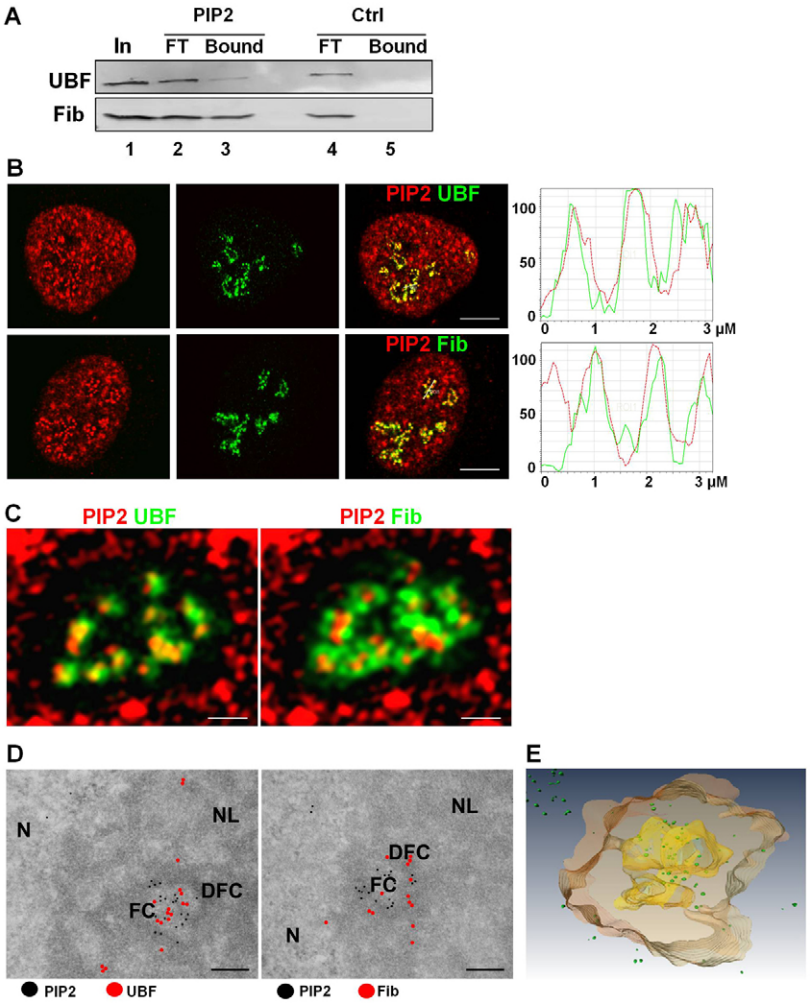

Fig. 3. PIP2 co-localizes with the Pol I transcription factor UBF and the rRNA early processing factor Fib in intact cells. (**A**) When nucleolar extract was incubated with PIP2-coupled agarose beads, UBF and Fib were found to be present in the PIP2-bound protein complex. [Lane 1, input; lane 2, protein unbound to PIP2-coupled agarose beads (flow-through); lane 3, protein pulled down with PIP2-coupled agarose beads; lane 4, protein unbound to control agarose beads (flow-through); lane 5, protein pulled down with control agarose beads.] In, input; FT, flow-through; Ctrl, control. (**B**) PLCδ1PH domain, used as a PIP2 marker, co-localized with UBF and Fib in U2OS cells. Scale bars: 5 μm. (**C**) SIM revealed PIP2 co-localization with UBF and Fib in the subnucleolar components, which can be identified as FC and DFC, respectively. Scale bars: 0.5 μm. (**D**) IEM precisely distinguished PIP2 co-localization with UBF inside and at the periphery of FC, and with Fib in the DFC of HeLa cells. N, nucleus; NL, nucleolus. Scale bars: 200 nm. (**E**) Ultrastructural architecture of PIP2 clusters in nucleolar subcompartments by TECNAI G2 20 LaB6 tomography. PIP2 is localized in HeLa cells using a pre-embedding procedure with 0.8 nm immunogold particles pseudocolored in green. The fibrillar center is pseudocolored in yellow, and the dense fibrillar component is in orange.

subnucleolar, due to its higher resolution as compared with confocal microscopy (Fig. 3C). In order to improve the resolution even further, immunoelectron microscopy (IEM) revealed PIP2 co-localization with UBF in the inner space of FCs where proteins involved in rDNA transcription reside, and on the border between FC and DFC where rDNA transcription takes place. PIP2-Fib co-localization was detected in the DFC region (Fig. 3D). To reveal the fine details of nucleolar compartmentalization in terms of PIP2 localization, 3D electron tomography was used, which demonstrated that PIP2-containing structures are found between individual FCs through the DFC and stretch out to the nucleoplasm as seen in Fig. 3E and in supplementary material Movie 1. These results support the data showing PIP2 involvement in rRNA biogenesis. In accordance with our previous observation showing the absence of B23 in PIP2 pull-down (Fig. 2E), PIP2 was not detected in GC, suggesting that PIP2 is not involved in the late maturation of pre-ribosome particles.

Even though proteins involved in ribosomal gene transcription and rRNA processing were shown to be interacting with PIP2, it was not clear if these interactions were direct. We therefore probed for direct interactions of PIP2 with recombinant UBF and Fib (Fig. 4A) on nitrocellulose membranes where PIP2 and PI4P were spotted. The results clearly showed direct binding of UBF and Fib to PIP2, but not to PI4P (Fig. 4B). As a control, we used recombinant OSH1PH domain (Fig. 4A), which binds to PI4P with high affinity (Roy and Levine, 2004), and importin 5 (Imp 5, Fig. 4A). OSH1PH was found to bind to PI4P with greater affinity than to PIP2, while Imp 5 did not show any binding to either PI4P or PIP2 (Fig. 4B). To clearly show direct protein–lipid interaction, we performed pull-down experiments with the recombinant proteins (UBF, Fib and Imp 5) using PIP2-coupled agarose beads and control agarose beads. Recombinant UBF and Fib were pulled down by PIP2, while Imp 5 failed to bind to PIP2 (Fig. 4C; supplementary material Fig. S6-1, Fig. S6-2, Fig. S6-3). In addition, trypsin digestion of UBF and Fib showed that PIP2 binding blocked a particular region of UBF for trypsin accessibility (Fig. 4D), while PIP2 binding to Fib resulted in higher accessibility for trypsin (Fig. 4E). These changes in digestion patterns point to the alteration of conformation or protection at certain sites of UBF and Fib due to binding to PIP2.

In order to understand the effect of PIP2 binding on UBF–rDNA interaction, a footprinting experiment was carried out by incubating purified recombinant UBF with PIP2, IP3 or DAG. Upon PIP2 binding, the overall binding of UBF to rDNA was reduced and a more selective footprint to the UBF binding sequence was observed (Fig. 4F, lane 4) compared with DAG (Fig. 4F, lane 2) or IP3 (Fig. 4F, lane 3). Normalized densitometric profiles of the footprint (left panel) show tighter binding of UBF with PIP2 at the UBF footprint sequence as compared with all the other conditions (Fig. 4F).

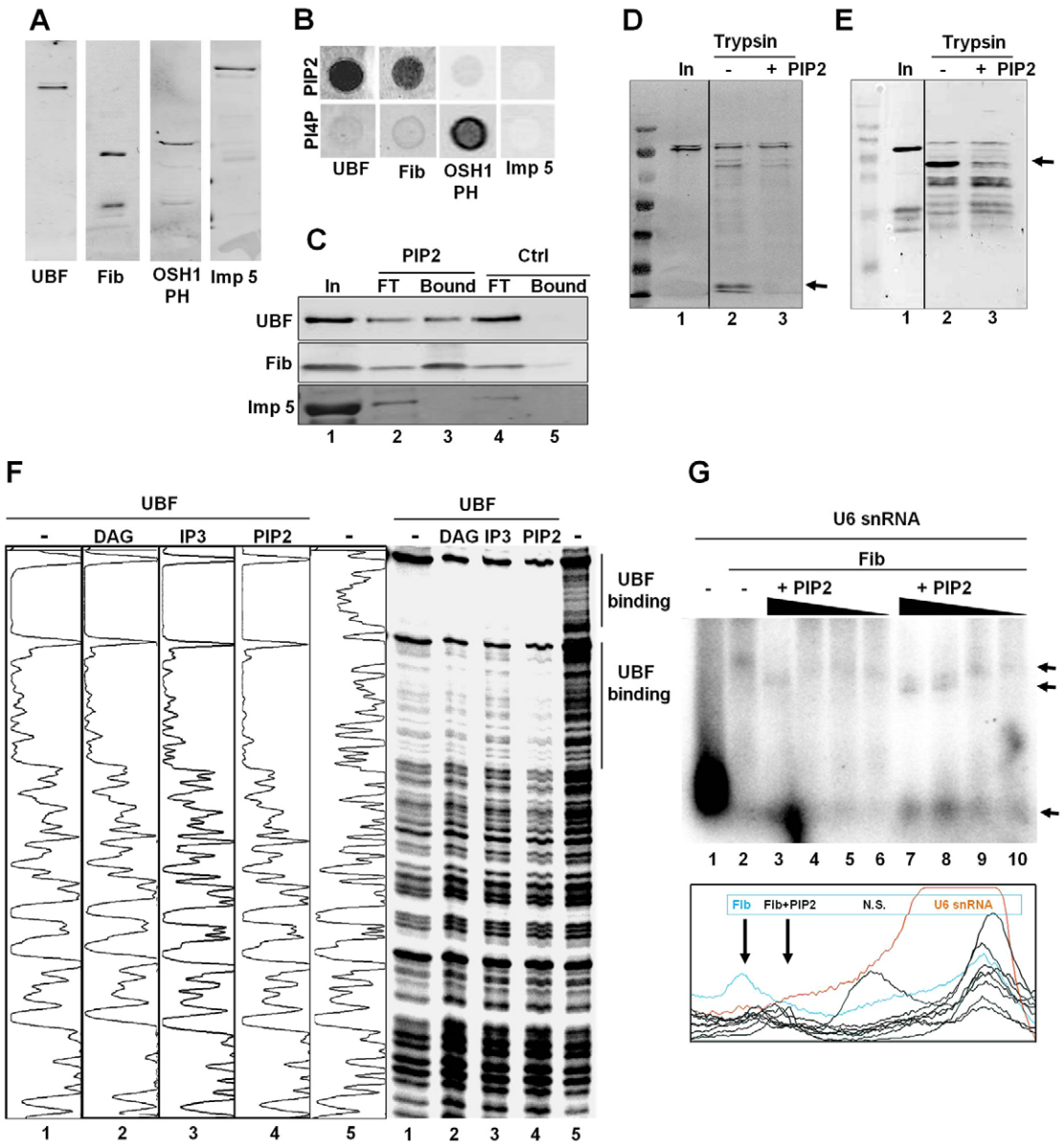

Fig. 4. UBF and Fib bind to PIP2 *in vitro*. (**A**) Western blot of purified UBF, Fib, OSH1PH and Imp 5 used in binding assays. (**B**) PIP2 and PI4P strips were incubated with recombinant UBF, Fib, OSH1PH and Imp 5 proteins for direct binding analysis. (**C**) Control agarose beads or PIP2-coupled agarose beads were incubated with purified UBF, Fib and Imp 5 proteins to study the direct binding to PIP2. [Lane 1, input; lane 2, protein unbound to PIP2-coupled agarose beads (flow-through); lane 3, protein pulled down with PIP2-coupled agarose beads; lane 4, protein unbound to control agarose beads (flow-through); lane 5, protein pulled down with control agarose beads.] In, input; FT, flow-through; Ctrl, control. (**D**) Limited protease digestion assays show a difference in the digestion pattern (arrow) of UBF due to a conformational change or specific binding of PIP2. (Lane 1, UBF as an input; lane 2, UBF treated with trypsin; lane 3, UBF treated with trypsin in the presence of PIP2.) (**E**) Limited protease digestion assays show a difference in digestion pattern of Fib (arrow) due to the conformational change or specific binding of PIP2. (Lane 1, Fib as an input; lane 2, Fib treated with trypsin; lane 3, Fib treated with trypsin in the presence of PIP2.) (**F**) A footprinting experiment was performed using purified recombinant UBF incubated with 100 ng DAG, IP3 and PIP2. (Lane 1, template incubated with UBF; lane 2, template incubated with UBF in the presence of DAG; lane 3, template incubated with UBF in the presence of IP3; lane 4, template incubated with UBF in the presence of PIP2; lane 5, template only.) UBF binding sites are indicated in the figure. Normalized densitometry plot analysis of the footprint is shown on the left. (**G**) PIP2 binding to Fib was tested by mobility assays with U6 snRNA where PIP2 association with Fib altered the mobility of RNA, suggesting an additional conformational bend or loop on RNA. [Lane 1, template; lane 2, template incubated with Fib; lanes 3–6, template incubated with Fib in the presence of decreasing amounts of PIP2 (0.1 µg, 0.05 µg, 0.025 µg, 0.0166 µg). Lanes 7–10 are the duplicates of lane 3–6, respectively. See supplementary material Fig. S7 for the entire gel pattern]. Different conformations of RNA–Fib complexes are reflected in the altered mobility of U6 snRNA shown by arrows. Normalized densitometry plot analysis of the gel shift shows Fib complex with U6 snRNA in blue, the Fib and PIP2 complex with U6 snRNA in black at different concentrations of PIP2 and U6 snRNA only as an orange plot. The peak marked as N.S. shows a nonspecific radioactive signal.

The influence of PIP2 on the binding of Fib to U6 small nuclear RNAs (snRNAs) was further investigated in gel shift mobility assays (Fig. 4G; supplementary material Fig. S7). The mobility of the Fib/U6 snRNA complex was altered in the gel during electrophoresis upon addition of PIP2, thus suggesting changes in RNA topology or other alterations resulting from PIP2 binding to Fib (Fig. 4G). Densitometric profile of the gel shift assay (below) clearly shows the increase in mobility of U6 snRNA/Fib complex upon binding to PIP2 as shown by the arrows at the peaks in the density profile (Fig. 4G).

PIP2 co-localizes with rRNA nascent transcripts in nucleoli

To assess the presence of PIP2 during early steps of rDNA transcription, we visualized nascent rRNA transcripts by short pulse incorporation of BrUTP in permeabilized cells. A clear co-localization between PIP2 and Br-rRNA was observed by immunofluorescence (Fig. 5A) and IEM (Fig. 5B). The labeling of nascent rRNA and PIP2 showed that both localize at the border between FC and DFC and in the DFC. PIP2 and Br-rRNA clusters were intermingled; most of the transcription signals were associated with PIP2 signal. However, there were also zones in DFC where only PIP2 labeling was present (Fig. 5B). These results demonstrate the presence of PIP2 at the sites of nucleolar transcription *in situ* and, in parallel with the *in vitro* data, show the importance of PIP2 for rDNA transcription and possibly nucleolar compartmentalization.

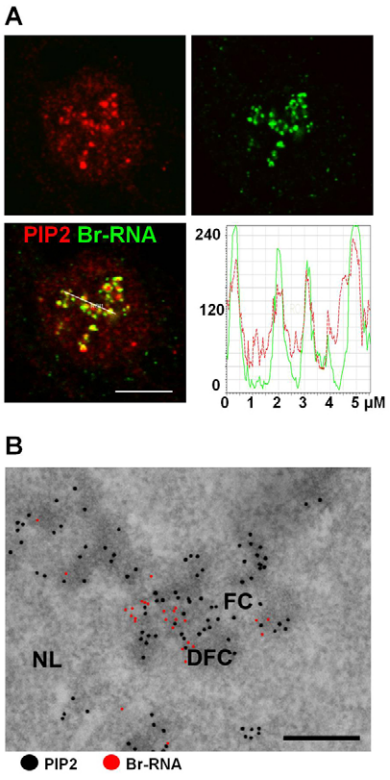

Fig. 5. PIP2 positive foci co-localize with rRNA nascent transcripts in nucleoli. (**A**) α-Amanitin treated U2OS cells showed very high co-localization of PIP2 and anti-BrdU positive nascent transcripts. Scale bar: 5 µm. (**B**) Immunogold detection revealed intermingled clusters and strings of PIP2 and rRNA transcripts in the DFC of HeLa cells. A major portion of Br-rRNA transcripts co-localized with PIP2 molecules, whereas some DFC zones contained only PIP2. NL, nucleolus. Scale bar: 200 nm.

Discussion

PIP2 is the source of the second messengers IP3 for intracellular Ca^{2+} mobilization and DAG for protein kinase C activation. In addition to the role of PIP2 in cytoplasmic signal transduction, the presence of its biosynthetic machinery inside the nucleus indicates a distinct nuclear signaling pathway (Irvine, 2003). The presence of phospholipids in the nucleus was shown more than 70 years ago (Stoneburg, 1939), however, little is known about their physico-chemical properties and functions in the nucleus. Since there are no membranous structures inside of the nucleus, it is suggested that proteins with hydrophobic pockets bind to PIPs to protect them from the hydrophilic environment (for review see Irvine, 2003). Here we demonstrate that PIP2 binds to some of the principal components of the Pol I transcription machinery and is anchored via these interactions in the fibrillar regions of the nucleolus where rDNA transcription occurs.

Over the years, only few studies reported the involvement of PIP2 in Pol II transcription. PIP2 addition was shown to promote Pol II transcription (Yu et al., 1998) and the binding of chromatin remodeling complex to DNA (Zhao et al., 1998). However, there have been no reports on the modulation of Pol I transcription by PIP2. Therefore, we first tested if PIP2 is required for Pol I transcription. Pol I transcription inhibition by the addition of either anti-PIP2 antibody or PLC enzyme indicated the involvement of PIP2 in Pol I transcription. We also observed a reduction in Pol I transcription upon depletion of PIP2, which was reversed by the addition of exogenous PIP2 to the depleted extract, but not by the addition of IP3 and DAG. Taken together, our data suggest that PIP2 acts as itself in Pol I transcription rather than as a substrate of nuclear PI-PLC, since neither IP3 nor DAG rescue the inhibitory effect of PIP2 depletion in Pol I transcription.

The presence of PIP2 on the Pol II promoter was recently shown by Toska et al. (Toska et al., 2012). BASP1 binding to PIP2 was shown to be required for the interaction with HDAC1, which resulted in the recruitment of HDAC1 to the promoter of WT1-targeted genes to repress transcription of Pol II (Toska et al., 2012). Here we report for the first time the presence of PIP2 in the transcription complex on the promoter during Pol I transcription. Pol I, UBF and Fib were detected in PIP2-bound protein complex while TBP and TAF 95/110 were not. This result indicates that instead of binding to the whole transcription machinery, PIP2 selectively binds to a subset of proteins involved in transcription. We found that PIP2 binds directly to UBF and they co-localize in FC region. UBF is a scaffold protein that binds to rDNA promoter and bends it to establish proper DNA–protein structure (Stefanovsky et al., 2001). According to the model proposed by Denissov et al. (Denissov et al., 2011), together with other components of SL1 complex, UBF creates a core-helix DNA structure where the transcribed regions are cylindrically wrapped around. Pol I initiates the transcription in the core and elongates along the cylindrical helix (Denissov et al., 2011). In addition, UBF is required for the formation of secondary constrictions of NORs (Mais et al., 2005). Since PIP2 binding to UBF results in a somewhat tighter binding to rDNA promoter, it is plausible that the interaction between PIP2 and UBF has a regulatory role in the formation of transcription initiation complex at the rDNA promoter.

Fib is known to have a role in nucleolar assembly by gathering prenuclear bodies together (Fomproix et al., 1998). Direct

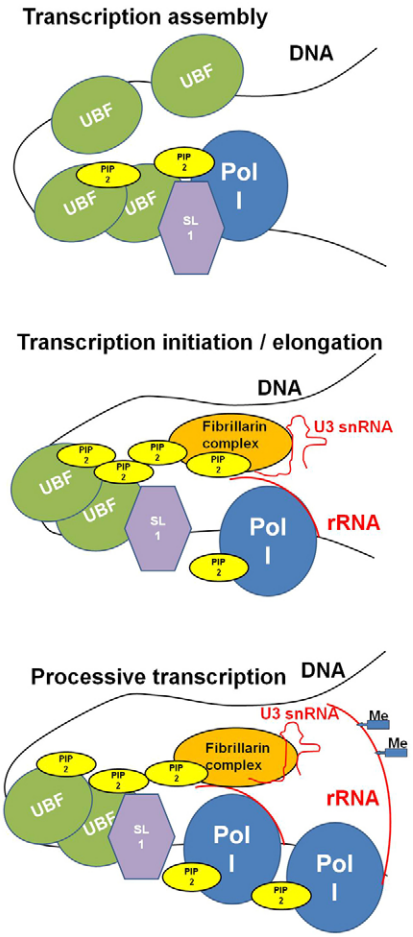

Fig. 6. Model for Pol I transcription. UBF and Pol I interacts with PIP2 during the transcription on the rDNA where PIP2 directs UBF to bind to a more specific site on the promoter compared with its promiscuous binding to the rDNA (transcription assembly). This specific promoter binding occurs in the FC/DFC region. Fib interacts with PIP2 only when RNA is newly synthesized and this interaction takes place in the DFC region close to UBF (transcription initiation/elongation). PIP2 is not involved in further processing of RNA and riboproteins since it is not localized in the GC region where maturation of rRNA takes place. Differences in the hydrophobicity of the complexes may have a role in the formation of subnucleolar structures (processive transcription).

binding of PIP2 to Fib caused an increase in the mobility of U6 snRNA/Fib complex, but did not significantly affect the amount of bound complex under the assay conditions. The change in mobility may arise from the altered physico-chemical properties of the complex due to PIP2 addition, or from conformational changes in Fib as suggested by the trypsin digestion in Fig. 4E. Similarly, it was reported that conformational opening of ezrin upon binding to PIP2 results in more extensive contacts with F-actin (Jayasundar et al., 2012). Since PIP2 localization is restricted to the transcriptionally active regions in the nucleolus, we suggest that a particular hydrophobic protein-lipid-RNA environment might exist in that particular region and contribute to the detergent-resistant nuclear PIP2 pools, which were shown to make up to 40% of the total PIP2 mass (Vann et al., 1997). The morphology of nuclear speckles was shown to be dependent on PIP2 binding to PDZ domain of syntenin-1 (Mortier et al., 2005). Therefore, it is likely that PIP2 also contributes to the formation of transcriptionally active sites of the nucleolus and acts as a structural interface between the nucleolar skeletal elements (like FC) and the macromolecular complexes involved in rDNA transcription and in early rRNA processing (FC/DFC interphase and DFC).

Our observation that nascent rRNA co-localizes with PIP2 contributes to a conclusion that PIP2 is associated with transcription machinery on active rDNA and has a role in Pol I transcription as well as in early stages of rRNA maturation. RNA was shown to be required for the localization of PIP2 to nuclear speckles (Osborne et al., 2001), and therefore it was suggested that the interaction with RNA/protein complex might stabilize PIP2 in the absence of intranuclear membranous structures. Similarly, PIP2 might be tethered within the nucleolus by the interaction with nascent rRNA transcripts and Fib, bridging the processes of nascent transcript production and early processing. To our knowledge, this is the first report on PIP2 involvement in Pol I transcription and rRNA processing.

All these findings led us to suggest a model in which PIP2 modulates UBF binding to rDNA, and Fib binding to rRNA. Upon active transcription Fib binds to PIP2 and associates with nascent rRNA in a Fib complex to enforce methylation for further rRNA processing. PIP2 may act as a bridge between Pol I, UBF and Fib to connect transcription initiation and early maturation steps. After the initial methylation, the Fib complex may release the rRNA to be further processed in the GC region (Fig. 6). The link between RNA synthesis and maturation may dictate nucleolar structures in the FC and DFC regions, where PIP2 may form a framework that allows gathering of proteins to work in concert for efficient transcription of rRNA genes.

Materials and Methods

Cell culture

Human osteosarcoma (U2OS) cells and cervical carcinoma (HeLa) cells were kept in DMEM with 10% fetal calf serum in 5% CO_2/air, 37℃, humidified atmosphere.

Plasmids

GST-tagged PLCδ1PH (1–140) (pGST3) and PLCδ1PH-Mut (R40A), which lacks binding to PIP2, were provided by Dr Hitoshi Yagisawa (Yagisawa et al., 1998). pECHU plasmid was constructed by PCR of the human rDNA promoter (−514 to +20) from prHU3 with *Eco*RI-*Xho*I site into pEC111/80 (Castaño et al., 2000) after the HIV LTR promoter removal. prHU3 was a kind gift from Dr Lucio Comai. UBF1 (gift from Dr Sui Huang) and Fib were cloned into pET15b vector for protein purification studies. In order to produce recombinant protein, OSH1PH domain (a gift from Dr Tamas Balla) was cloned into pET42a(+) vector. Imp 5 in pQE30 vector was received from Dr Dirk Görlich (Jäkel and Görlich, 1998).

Expression and purification of recombinant proteins

Recombinant Fib, UBF, PLCδ1PH and PLCδ1PH-Mut were expressed in *Escherichia coli (E. coli)* BL21 (DE3)-pLysS (Stratagene, La Jolla, CA, USA). Both UBF and Fib had histidine tags and were purified over Ni-agarose in a buffer (20 mM Tris pH 8, 0.1 mM EDTA, 20% glycerol, 500 mM NaCl, 0.1% NP40, 1 mM DTT). UBF was further purified by passing through a Q Sepharose fast flow column (17-0510-10, GE Healthcare, Uppsala, Sweden) followed by a SP Sepharose fast flow column (17-0729-10, GE Healthcare, Uppsala, Sweden). For GST-tagged PLCδ1PH and PLCδ1PH-Mut, the purification was carried on glutathione–agarose column (G4510, Sigma Aldrich, St. Louis, MO, USA), which had been equilibrated with BC100 (20 mM Tris pH 8, 0.1 mM EDTA, 20% glycerol, 100 mM NaCl). Proteins were eluted with 50 mM Tris-HCl, pH 8 having 0.1 g reduced L-Glutathione (G4251, Sigma Aldrich, St. Louis, MO, USA).

11 mg of partially purified PLC from *Clostridium perfringens* (*C. welchii*) (P7633-125 UN, Sigma Aldrich, St. Louis, MO, USA) was further purified by passing through a SP Sepharose fast flow column followed by a Q Sepharose fast flow column. Proteins were eluted in a KCl gradient at 500 mM.

Recombinant OSH1PH domain was expressed in Rosetta™(DE3)pLysS competent cells (70956, Millipore EMD, Billerica, MA, USA) and purified over glutathione–agarose column followed by Ni-agarose column. Elution from

Ni-agarose column was performed in a buffer consisted of 25 mM HEPES, pH 8, 100 mM NaCl and 250 mM imidazole.

Recombinant Imp 5 was expressed in Qiagen Rep4 strain of *E. coli* and purified over Ni-agarose column as described previously (Kutay et al., 1997).

Confocal microscopy

Primary antibodies: Anti-GST antibody (gift from Dr Igor Shevelev; 5 μg/ml), anti-PIP2 antibody (2C11, Abcam, Cambridge, UK; 16 μg/ml), anti-Fib antibody (38F3, Abcam, Cambridge, UK; dilution 1:100), anti-UBF antibody (sc13125, Santa Cruz Biotechnology, Inc., CA, USA; 2 μg/ml), anti-RPA116 antibody (gift from Dr Ingrid Grummt; 2 μg/ml). Secondary antibodies: Donkey anti-mouse IgG conjugated with Alexa 488 (Invitrogen, CA, USA), goat anti-rabbit IgG conjugated with Alexa 647 (Invitrogen, CA, USA) and donkey anti-mouse IgM conjugated with Cy3 (Jackson ImmunoResearch Laboratories Inc., West Grove, PA, USA). Images were taken using a confocal microscope (Leica TCS SP5 AOBS TANDEM, Germany) with a 100× (NA 1.4) oil immersion objective lens. In order to test the specificity of the primary antibodies, anti-UBF, anti-Fib and anti-PIP2 antibodies were preblocked with an excess amount of purified UBF, Fib and PIP2, respectively. Preblocking incubations were performed in PBS with 1% BSA. After 30 min incubation, immunostaining was performed with these preblocked primary antibodies.

IEM

Primary antibodies used in IEM were already described in confocal microscopy section. Secondary antibodies: Goat anti-mouse IgG (H^+L chains) antibody coupled with 6 nm colloidal gold particles, goat anti-mouse IgM (μ-chain specific) antibody coupled with 12 nm colloidal gold particles, goat anti-rabbit IgG (H^+L chains) antibody coupled with either 6 nm or 12 nm colloidal gold particles (Jackson ImmunoResearch Laboratories Inc., West Grove, PA, USA). The thin sections (70–90 nm) were examined by a FEI Morgagni 268 transmission electron microscope at 80 kV. The images were captured with Mega View III CCD camera. Multiple sections of at least three independent immunogold labeling experiments were analyzed.

Detection of transcription sites by confocal microscopy and IEM

Bromouridine triphosphate (BrUTP; Sigma Aldrich, St. Louis, MO, USA) incorporation was performed as described previously (Pombo et al., 1999). For Br-RNA labeling anti-bromodeoxyuridine antibody IgG1 (BMC9318, Roche Diagnostics GmbH, Mannheim, Germany; 20 μg/ml) was used.

SIM

Images were taken with a super-resolution structured illumination microscope (ELYRA PS.1, Carl Zeiss, Munich, Germany) with Plan-Apochromat 63×/1.4 Oil DIC M27 oil immersion objective lens using the parameters as follows: number of SIM rotations, 5; SIM grating periods varied according to the excitation wavelength from 34.0 μm to 42.0 μm.

PIP strips

Purified UBF, Fib, OSH1PH domain and Imp 5 were tested on PIP Strips (Echelon Biosciences Inc., CA, USA). The membranes were blocked with 5 ml of blocking buffer (PBST, 3% BSA) for 1 h at RT. UBF and Fib were added in 5 ml blocking buffer overnight at 4℃. After binding, membranes were washed three times with PBST and followed the same protocol as western blots.

Limited protease digestion assay

Purified UBF (100 ng) and Fib (200 ng) were incubated for 30 min at RT with or without PIP2 (1 μg) in BC100 buffer. After the incubation, trypsin (0.5 ng) was added and the mixtures were incubated for 1 min at 4℃, as indicated. The digestion reactions were stopped by adding 10 μl Laemmli buffer (0.25 M Tris, pH 6.8, 20% glycerol, 5% mercaptoethanol, 2% SDS, 0.025% Bromophenol Blue) and the samples were denatured at 95℃ for 5 min, electrophoresed through a 15% SDS-PAGE. Western blot was carried out as described previously.

Footprint

10 ng of radioactively end labeled PCR reactions from rDNA −514 to 100 from prHU3 were used as template for binding to purified UBF (100 ng) in the presence or absence of added compounds with the amounts mentioned in the legends for 30 min at 4℃ in a buffer containing 20 mM Tris pH 7.4, 1 μg pUC 18, 5% glycerol, protease inhibitors. After binding, the reactions were digested with 1 unit of DNase I (Fermentas, MA, USA) for 1 min at 4℃, followed by phenol/chloroform extraction and ethanol precipitation. Purified DNA was run on a 6% PAGE with 6M urea. Footprint image was analyzed as previously published (Hofmann et al., 2011). For quantitative analysis of the footprint, ImageJ 1.42q software was used. We normalized the plot using the measurements from the non-UBF binding region of the footprint for each lane.

Gel shift

Radioactively labeled U6 snRNA (40 Kcpm, gift from Dr Gary R. Kunkel) was used as a template for binding to purified Fib (200 ng). The reactions were incubated on ice for 30 min then loaded onto a 1% agarose gel and ran in cold room for 2 h at 40 V. Bands were visualized by autoradiography. For quantitative analysis of the gel shift, ImageJ 1.42q software was used. Photoshop was used to assign a particular color for each plot profile and compiled into one plot for easier comparison.

In vitro pull-down of PIP2

Nuclear and nucleolar lysates were prepared from HeLa cells as previously described (Andersen et al., 2002). Nuclear lysates were incubated with glutathione agarose beads (G4510, Sigma Aldrich, St. Louis, MO, USA) in the presence of GST-tagged PLCδ1PH and PLCδ1PH-Mut for 2 h or overnight at 4℃ and washed thoroughly with 10 mM HEPES pH 7.9, 1 mM $MgCl_2$, 0.5 mM DTT. Nuclear and nucleolar lysates were incubated with control agarose beads or agarose beads coupled with PIP2 (Echelon Biosciences Inc., CA, USA) for 2 h at 4℃ and thoroughly washed with RIPA buffer (50 mM Tris, pH 7.5, 150 mM NaCl, 1% NP-40, 0.5% DTT and protease inhibitors). Beads were boiled in Laemmli buffer for 5 min and resolved by SDS-PAGE for immunoblotting detection. In order to check direct interactions between proteins and PIP2, recombinant proteins (~2 μg of recombinant protein used in each incubation) were incubated with control agarose beads or PIP2-coupled agarose beads which were previously blocked with 1% BSA in PBS. The beads were then thoroughly washed with BC100 buffer and were boiled in Laemmli buffer for 5 min and resolved by SDS-PAGE for immunoblotting detection.

In vitro transcription assays

Run-off transcription assays were performed using HeLa nuclear extracts or HeLa nuclear extracts depleted for PIP2 using PLCδ1PH coated beads and as a control PLCδ1PH-Mut coated beads used for depletion. The reactions contained 15 mM HEPES pH 7.9, 100 mM KCl, 5 mM $MgCl_2$, 10% glycerol, 1 mM DTT, 0.1 mM EDTA, 100 μg/ml of α-amanitin, 100 mg/ml β-cyclodextrin, in the presence or absence of added compounds with the amounts mentioned in the legends. Extracts were incubated at 25℃ for 20 min before initiating the transcription reaction by adding 500 μM ATP, GTP, CTP, 50 μM UTP, [α-^{32}P] UTP (8 Ci/mmol) and 100 ng of prHU3 plasmid digested with *Sal*I endonuclease. PLC was added before or after nucleotides as stated in the figure legend. The reactions were incubated for 1 h at 30℃ and transcripts were purified by phenol extraction and ethanol precipitation. The RNA was electrophoretically resolved on a 6% acrylamide sequencing gel with 6M urea and visualized and quantified with a PhosphorImager. For quantitative measurement of each band, background was subtracted and each lane was normalized to a labeled primer, which was added as an internal loading control. The data were compared in two independent experiments. Having set the initial control condition at 100%, the plots represent the mean of each measurement and standard error of the mean for each condition.

In order to assay if PIP2 was bound to the transcription machinery on the promoter during the *in vitro* transcription, rDNA promoter region was produced by using biotinylated F-primer 5′-CCAACGCGTTGGATGCATAGCTT-3′ and R-primer 5′-ATCCTTTTTGATAATCTCATGACC-3′, bound to streptavidin coupled magnetic beads (Dynabeads MyOne Streptavidin C1, 650.01, Invitrogen, CA, USA) and blocked with 5% BSA. The beads were then incubated with HeLa nuclear extract in a transcription buffer without nucleotides. For PIP2 detection purified PLCδ1PH or PLCδ1PH-Mut domains were also added to the nuclear extracts. The beads were incubated with nuclear extracts for 1 h. After incubation of the beads, half of the reactions were allowed to transcribe in the presence of only ATP or all the rNTPs to distinguish between transcription initiation and elongation, respectively. Afterwards, the beads were washed six times with wash buffer and loaded onto a SDS-PAGE for western blot analysis.

Thin layer chromatography for PIP2 in cell free system

In vitro transcription reactions were carried out using rDNA promoter region or control DNA which is a part of the vector pGEM7z+ bound to magnetic beads and blocked with 5% BSA. The beads were then incubated with nuclear extract in a transcription buffer with only ATP or all the rNTPs. After transcription, the beads were washed and lipid extractions were processed. We used an earlier published protocol (Yu et al., 1998) to extract PIP2 from bound protein followed by loading on TLC plates that were gently soaked in 1% (w/v) potassium oxalate and dried. The solution for separation was 90:90:7:22 ($CHCl_3$:MeOH:NH_3OH:H_20; v/v/v/v). TLC was then stained with acidic phosphomolybdate solution.

3D electron tomography of PIP2 in nucleolus

For 3D electron tomography, HeLa cells were grown on coverslips and fixed with 4% PFA for 15 min, permeabilized in 0.5% Triton X-100 for 5 min, washed in PBS and blocked in the mixture of 5% BSA, 5% NGS and 0.1% fish gelatin for 10 min. Then, cells were washed with the incubation buffer (0.1% BSA, pH 7.4) and incubated with a primary antibody overnight at +4℃. After thorough washes, cells were incubated with a secondary antibody conjugated to ultra-small (0.8 nm) gold particles (Aurion, Wageningen, The Netherlands). Then, cells were washed in

the incubation buffer, additionally fixed in 2% glutaraldehyde, washed in distilled water and silver-enhanced using the Aurion kit for 45 min. After washing in distilled water, cells were dehydrated in ethanol series and embedded in Epon resin by standard procedure. 400-nm sections were cut with ultra microtome for single-axis electron tomography. The tilt series were acquired using TECNAI G2 20 LaB6 electron microscope (FEI, Eindhoven, The Netherlands) operated at 200 kV. The tilt series were aligned using the Inspect 3D software (FEI). Visualization was done using the Amira software (Visage Imaging GmbH, Berlin, Germany).

Acknowledgements

We thank Pavel Kříž, Iva Jelínková and Ivana Nováková for excellent technical assistance. We thank Anatolij A. Philimonenko and Karel Janoušek for their help with 3D tomography. We thank Dr Sui Huang, Dr D. Hernandez-Verdun, Dr Hitoshi Yagisawa, Dr Tamas Balla, Dr Lucio Comai, Dr Igor Shevelev, Dr Ingrid Grummt and Dr Gary R. Kunkel for sharing plasmids and antibodies with us. We also thank Dr Jacques Paysan for his help with SIM.

Author contributions

S.Y., E.C. and P.H. conceived and designed the experiments. S.Y., E.C., M.S., V.V.P., R.D. and T.V. performed the experiments. S.Y., E.C., M.S., P.H., V.V.P., R.D. and T.V. analyzed the data. S.Y., E.C. and P.H. wrote the paper.

Funding

This work was supported by the Grant Agency of the Czech Republic [grant numbers P305/11/2232, 204/09/H084]; the Ministry of Education, Youth and Sports of the Czech Republic [grant numbers LC545, LC06063]; CONACYT [grant number 176598]; and the Institute of Molecular Genetics, Academy of Sciences of the Czech Republic [institutional grant number RVO68378050].

Supplementary material available online at
http://jcs.biologists.org/lookup/suppl/doi:10.1242/jcs.123661/-/DC1

References

Andersen, J. S., Lyon, C. E., Fox, A. H., Leung, A. K., Lam, Y. W., Steen, H., Mann, M. and Lamond, A. I. (2002). Directed proteomic analysis of the human nucleolus. *Curr. Biol.* **12**, 1-11.

Anderson, S. J., Sikes, M. L., Zhang, Y., French, S. L., Salgia, S., Beyer, A. L., Nomura, M. and Schneider, D. A. (2011). The transcription elongation factor Spt5 influences transcription by RNA polymerase I positively and negatively. *J. Biol. Chem.* **286**, 18816-18824.

Boronenkov, I. V., Loijens, J. C., Umeda, M. and Anderson, R. A. (1998). Phosphoinositide signaling pathways in nuclei are associated with nuclear speckles containing pre-mRNA processing factors. *Mol. Biol. Cell* **9**, 3547-3560.

Castaño, E., Gross, P., Wang, Z., Roeder, R. G. and Oelgeschläger, T. (2000). The C-terminal domain-phosphorylated IIO form of RNA polymerase II is associated with the transcription repressor NC2 (Dr1/DRAP1) and is required for transcription activation in human nuclear extracts. *Proc. Natl. Acad. Sci. USA* **97**, 7184-7189.

Cheng, M. K. and Shearn, A. (2004). The direct interaction between ASH2, a Drosophila trithorax group protein, and SKTL, a nuclear phosphatidylinositol 4-phosphate 5-kinase, implies a role for phosphatidylinositol 4,5-bisphosphate in maintaining transcriptionally active chromatin. *Genetics* **167**, 1213-1223.

Cocco, L., Gilmour, R. S., Ognibene, A., Letcher, A. J., Manzoli, F. A. and Irvine, R. F. (1987). Synthesis of polyphosphoinositides in nuclei of Friend cells. Evidence for polyphosphoinositide metabolism inside the nucleus which changes with cell differentiation. *Biochem. J.* **248**, 765-770.

Denissov, S., Lessard, F., Mayer, C., Stefanovsky, V., van Driel, M., Grummt, I., Moss, T. and Stunnenberg, H. G. (2011). A model for the topology of active ribosomal RNA genes. *EMBO Rep.* **12**, 231-237.

Divecha, N., Banfić, H. and Irvine, R. F. (1991). The polyphosphoinositide cycle exists in the nuclei of Swiss 3T3 cells under the control of a receptor (for IGF-I) in the plasma membrane, and stimulation of the cycle increases nuclear diacylglycerol and apparently induces translocation of protein kinase C to the nucleus. *EMBO J.* **10**, 3207-3214.

Dundr, M., Meier, U. T., Lewis, N., Rekosh, D., Hammarskjöld, M. L. and Olson, M. O. (1997). A class of nonribosomal nucleolar components is located in chromosome periphery and in nucleolus-derived foci during anaphase and telophase. *Chromosoma* **105**, 407-417.

Fomproix, N., Gébrane-Younès, J. and Hernandez-Verdun, D. (1998). Effects of anti-fibrillarin antibodies on building of functional nucleoli at the end of mitosis. *J. Cell Sci.* **111**, 359-372.

Hernandez-Verdun, D. (1991). The nucleolus today. *J. Cell Sci.* **99**, 465-471.

Hofmann, N., Wurm, R. and Wagner, R. (2011). The E. coli anti-sigma factor Rsd: studies on the specificity and regulation of its expression. *PLoS ONE* **6**, e19235.

Irvine, R. F. (2003). Nuclear lipid signalling. *Nat. Rev. Mol. Cell Biol.* **4**, 349-360.

Jäkel, S. and Görlich, D. (1998). Importin beta, transportin, RanBP5 and RanBP7 mediate nuclear import of ribosomal proteins in mammalian cells. *EMBO J.* **17**, 4491-4502.

Jayasundar, J. J., Ju, J. H., He, L., Liu, D., Meilleur, F., Zhao, J., Callaway, D. J. and Bu, Z. (2012). Open conformation of ezrin bound to phosphatidylinositol 4,5-bisphosphate and to F-actin revealed by neutron scattering. *J. Biol. Chem.* **287**, 37119-37133.

Kopp, K., Gasiorowski, J. Z., Chen, D., Gilmore, R., Norton, J. T., Wang, C., Leary, D. J., Chan, E. K., Dean, D. A. and Huang, S. (2007). Pol I transcription and pre-rRNA processing are coordinated in a transcription-dependent manner in mammalian cells. *Mol. Biol. Cell* **18**, 394-403.

Kutay, U., Izaurralde, E., Bischoff, F. R., Mattaj, I. W. and Görlich, D. (1997). Dominant-negative mutants of importin-beta block multiple pathways of import and export through the nuclear pore complex. *EMBO J.* **16**, 1153-1163.

Liau, M. C. and Perry, R. P. (1969). Ribosome precursor particles in nucleoli. *J. Cell Biol.* **42**, 272-283.

Mais, C., Wright, J. E., Prieto, J.-L., Raggett, S. L. and McStay, B. (2005). UBF-binding site arrays form pseudo-NORs and sequester the RNA polymerase I transcription machinery. *Genes Dev.* **19**, 50-64.

Mayer, C. and Grummt, I. (2006). Ribosome biogenesis and cell growth: mTOR coordinates transcription by all three classes of nuclear RNA polymerases. *Oncogene* **25**, 6384-6391.

Mellman, D. L., Gonzales, M. L., Song, C., Barlow, C. A., Wang, P., Kendziorski, C. and Anderson, R. A. (2008). A PtdIns4,5P2-regulated nuclear poly(A) polymerase controls expression of select mRNAs. *Nature* **451**, 1013-1017.

Mortier, E., Wuytens, G., Leenaerts, I., Hannes, F., Heung, M. Y., Degeest, G., David, G. and Zimmermann, P. (2005). Nuclear speckles and nucleoli targeting by PIP2-PDZ domain interactions. *EMBO J.* **24**, 2556-2565.

Németh, A. and Längst, G. (2011). Genome organization in and around the nucleolus. *Trends Genet.* **27**, 149-156.

Okada, M., Jang, S. W. and Ye, K. (2008). Akt phosphorylation and nuclear phosphoinositide association mediate mRNA export and cell proliferation activities by ALY. *Proc. Natl. Acad. Sci. USA* **105**, 8649-8654.

Osborne, S. L., Thomas, C. L., Gschmeissner, S. and Schiavo, G. (2001). Nuclear PtdIns(4,5)P2 assembles in a mitotically regulated particle involved in pre-mRNA splicing. *J. Cell Sci.* **114**, 2501-2511.

Pombo, A., Jackson, D. A., Hollinshead, M., Wang, Z., Roeder, R. G. and Cook, P. R. (1999). Regional specialization in human nuclei: visualization of discrete sites of transcription by RNA polymerase III. *EMBO J.* **18**, 2241-2253.

Rando, O. J., Zhao, K., Janmey, P. and Crabtree, G. R. (2002). Phosphatidylinositol-dependent actin filament binding by the SWI/SNF-like BAF chromatin remodeling complex. *Proc. Natl. Acad. Sci. USA* **99**, 2824-2829.

Rose, H. G. and Frenster, J. H. (1965). Composition and metabolism of lipids within repressed and active chromatin of interphase lymphocytes. *Biochim. Biophys. Acta* **106**, 577-591.

Roy, A. and Levine, T. P. (2004). Multiple pools of phosphatidylinositol 4-phosphate detected using the pleckstrin homology domain of Osh2p. *J. Biol. Chem.* **279**, 44683-44689.

Schneider, D. A., French, S. L., Osheim, Y. N., Bailey, A. O., Vu, L., Dodd, J., Yates, J. R., Beyer, A. L. and Nomura, M. (2006). RNA polymerase II elongation factors Spt4p and Spt5p play roles in transcription elongation by RNA polymerase I and rRNA processing. *Proc. Natl. Acad. Sci. USA* **103**, 12707-12712.

Schneider, D. A., Michel, A., Sikes, M. L., Vu, L., Dodd, J. A., Salgia, S., Osheim, Y. N., Beyer, A. L. and Nomura, M. (2007). Transcription elongation by RNA polymerase I is linked to efficient rRNA processing and ribosome assembly. *Mol. Cell* **26**, 217-229.

Stefanovsky, V. Y., Pelletier, G., Bazett-Jones, D. P., Crane-Robinson, C. and Moss, T. (2001). DNA looping in the RNA polymerase I enhancesome is the result of non-cooperative in-phase bending by two UBF molecules. *Nucleic Acids Res.* **29**, 3241-3247.

Stoneburg, C. A. (1939). The lipids of the cell nuclei. *J. Biol. Chem.* **129**, 189-196.

Toska, E., Campbell, H. A., Shandilya, J., Goodfellow, S. J., Shore, P., Medler, K. F. and Roberts, S. G. (2012). Repression of transcription by WT1-BASP1 requires the myristoylation of BASP1 and the PIP2-dependent recruitment of histone deacetylase. *Cell Rep.* **2**, 462-469.

Vann, L. R., Wooding, F. B., Irvine, R. F. and Divecha, N. (1997). Metabolism and possible compartmentalization of inositol lipids in isolated rat-liver nuclei. *Biochem. J.* **327**, 569-576.

Watt, S. A., Kular, G., Fleming, I. N., Downes, C. P. and Lucocq, J. M. (2002). Subcellular localization of phosphatidylinositol 4,5-bisphosphate using the pleckstrin homology domain of phospholipase C delta1. *Biochem. J.* **363**, 657-666.

Yagisawa, H., Sakuma, K., Paterson, H. F., Cheung, R., Allen, V., Hirata, H., Watanabe, Y., Hirata, M., Williams, R. L. and Katan, M. (1998). Replacements of single basic amino acids in the pleckstrin homology domain of phospholipase C-delta1 alter the ligand binding, phospholipase activity, and interaction with the plasma membrane. *J. Biol. Chem.* **273**, 417-424.

Yu, H., Fukami, K., Watanabe, Y., Ozaki, C. and Takenawa, T. (1998). Phosphatidylinositol 4,5-bisphosphate reverses the inhibition of RNA transcription caused by histone H1. *Eur. J. Biochem.* **251**, 281-287.

Zhao, K., Wang, W., Rando, O. J., Xue, Y., Swiderek, K., Kuo, A. and Crabtree, G. R. (1998). Rapid and phosphoinositol-dependent binding of the SWI/SNF-like BAF complex to chromatin after T lymphocyte receptor signaling. *Cell* **95**, 625-636.

Journal of Cell Science

Fig. S1. Preincubation of PIP2 with anti-PIP2 antibody neutralizes the inhibitory effect of antibody in Pol I transcription. Run-off transcription reaction showed that PIP2 blocked the inhibitory effect of anti-PIP2 antibody (clone 2C11, Abcam, Cambridge, UK; 0.8 μg) in transcription in a dose-dependent manner. (Lane 1: control transcription reaction; lane 2: transcription reaction in the presence of anti-PIP2 antibody; lane 3 and 4: transcription reaction in the presence of anti-PIP2 antibody with the addition of 50 ng and 100 ng PIP2, respectively).

Fig. S2. Ponceau staining of blotted proteins from in vitro pull-down wherein recombinant Wt and Mut PLCδ1PH domains were incubated with nuclear lysates.

Fig. S3. Ponceau staining of blotted proteins from in vitro pull-down performed by incubation of nuclear lysate with control agarose beads or PIP2-coupled agarose beads.

Fig. S4. Ponceau staining of blotted proteins from in vitro pull-down performed by incubation of nucleolar lysate with control agarose beads or PIP2-coupled agarose beads.

Fig. S5. Control experiment showing the specificity of the antibodies used. Specific signals were diminished after blocking the primary antibodies with excess amount of relevant proteins or lipids. When primary antibodies were omitted, secondary antibodies did not produce any visible signal. Scale bar: 5 μm.

Fig. S6-1,2,3. Ponceau staining of blotted proteins from in vitro pull-down experiments performed by incubation of control agarose beads or PIP2-coupled agarose beads with purified UBF, Fib and Imp 5 proteins, respectively.

Fig. S7. Gel shift assay in which aggregates formed after fibrillarin addition can be seen in the wells. This aggregation leads to an apparent loss of radioactivity in the corresponding gel lanes.

Supplementary Figures

Fig. S1

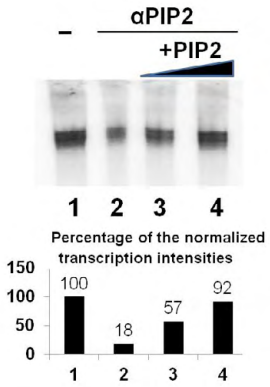

Fig. S2

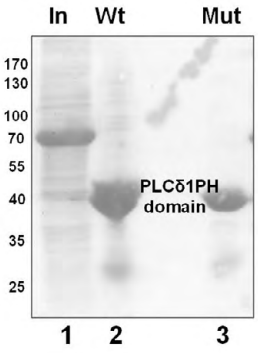

Fig. S3

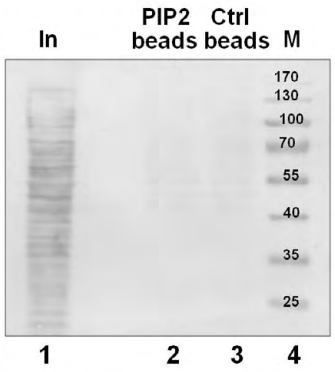

Fig. S4

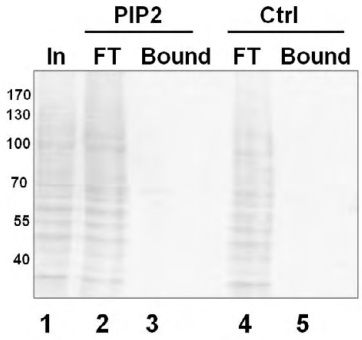

Fig. S5

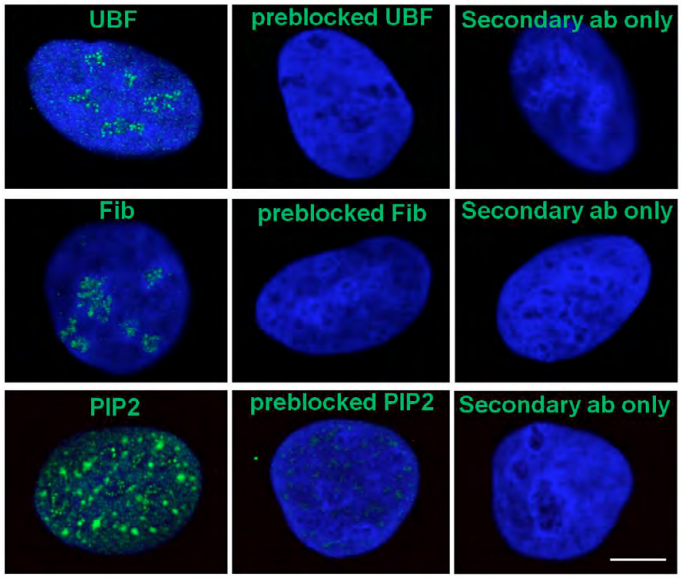

Fig. S6-1

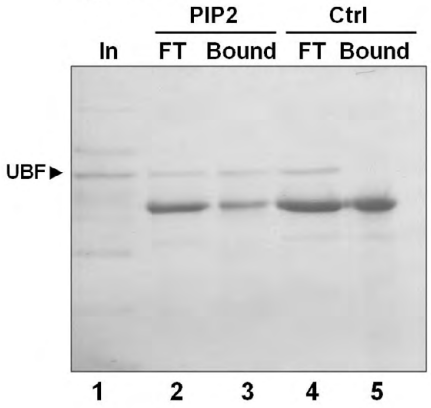

Fig. S6-2

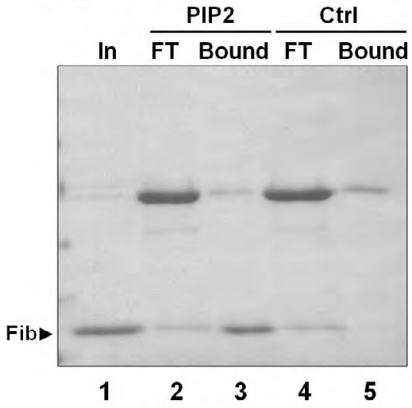

Fig. S6-3

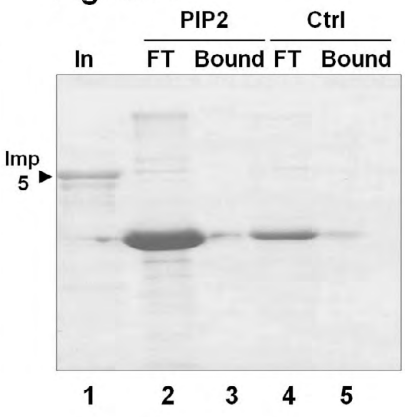

Fig. S7

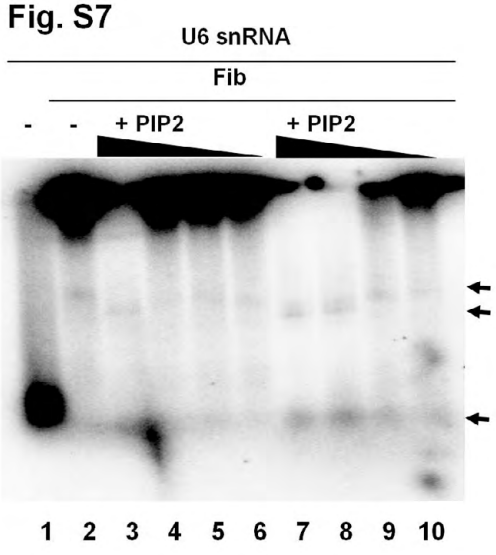

Movie 1. PIP2 localization in nucleolus by 3D electron tomography. Ultrastructural architecture of PIP2-clusters in nucleolar subcompartments by TECNAI G2 20 LaB6 tomography. PIP2 is localized using pre-embedding procedure with 0.8 nm immunogold particles pseudocoloured in green. Fibrillar center is pseudocoloured in yellow, dense fibrillar component is pseudocoloured in orange.